2013. Proceedings of the Indiana Academy of Science 122(2):118–125

STRUCTURAL VIBRATIONS: NORMAL MODES IN A HAND-BELL

Uwe J. Hansen: Department of Chemistry and Physics, Indiana State University, Terre Haute, IN 47809

ABSTRACT. The vibrational modes contributing most significantly to the radiated sound of hand-bells, are the bending waves travelling along the bell surface with periodic boundary conditions in the angular direction, nearly clamped boundaries near the crown, and free boundary conditions at the mouth of the bell. They are usually identified by two indices (m,n), where m counts the number of nodal lines crossing the crown, and n the number of circumferential nodal lines. The (m,0) modes, for values of m higher than a critical value, are missing. They are replaced by a mode for which the first circumferential nodal line lies very close to the mouth of the bell. These modes are designated as (m,$1^{\#}$) modes. Using Finite Element Analysis (FEA) a hand-bell is modeled with increasing complexity to show that both positive and negative curvatures are required in the bell wall to account for the presence of the (m,$1^{\#}$) modes.

Keywords: Normal modes, nodal lines, hand-bell, boundary condition, Finite Element Analysis (FEA)

INTRODUCTION

The partial differential equation in space and time associated with a local disturbance in an infinite medium, generally is a wave equation with solutions representing traveling waves. Imposing boundary conditions usually limits the possible solutions to a discrete set of standing waves identified with normal modes of vibration. The shape of a hand-bell naturally forms a free boundary at the mouth of the bell, whereas the crown essentially clamps the bell wall, imposing a condition of no translational or rotational motion at the top of the bell.

Experimental studies on hand-bells by T. D. Rossing, R. Perrin, H. J. Sathoff, and R. W. Peterson[1] include holographic interference patterns shown in figure 1.

Systematic grouping of those images by T. D. Rossing and R. Perrin[2] gives a periodic table-like representation shown in figure 2.

Figure 3[1] shows a systematic relationship between the frequency and the first mode index m, identifying the number of nodal lines crossing the crown, on logarithmic scales.

From all of these illustrations it becomes apparent that the (m,$1^{\#}$) modes naturally fall into the sequence of (m,0) modes. This paper uses FEA modeling to investigate which bell characteristics are responsible for the transition from (m,0) to (m,$1^{\#}$) modes. FEA solutions also include torsional and extensive modes, which will not be considered in this paper. This paper is limited to the study of transverse bending waves.

As a starting point, reference is made to the solution of a one dimensional wave equation for an elastic string under tension, where hinged boundary conditions at the ends limit the solutions to standing waves in the form of integral numbers of loops. Weinreich[3] shows, that relaxing the hinged condition at one end to make it either more spring-like or more mass-like, results in either an open end, or a fish-tail-like configuration respectively (figure 4).

It is not entirely unreasonable to expect a two dimensional extension of that model for a clamped top with hinged boundaries at the side and a free bottom, to result in an effective relaxing of the boundary, yielding an (m,$1^{\#}$) mode. This suggests that for sufficiently narrow plates, a strictly free boundary is not compatible with the hinged boundary on the sides, resulting in a fish-tail-like configuration at the open end in the two dimensional extension of the Weinreich one-dimensional model, corresponding to the (m,$1^{\#}$) modes for a sufficiently narrow mode section.

Corresponding author: Uwe J. Hansen, Dept. of Chem & Physics, Indiana State University, Terre Haute, IN (e-mail: uwe.hansen@indstate.edu. 812-234-0229).

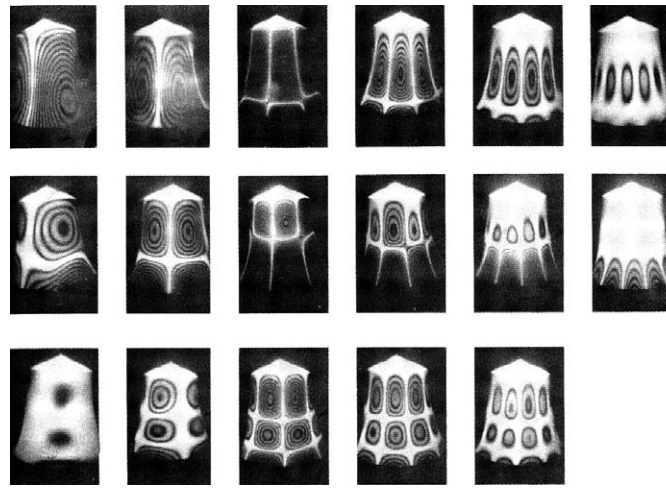

Figure 1.—Vibrational modes of a hand-bell imaged with holographic interferometry (from Rossing, Perrin, Sathoff & Peterson[1]).

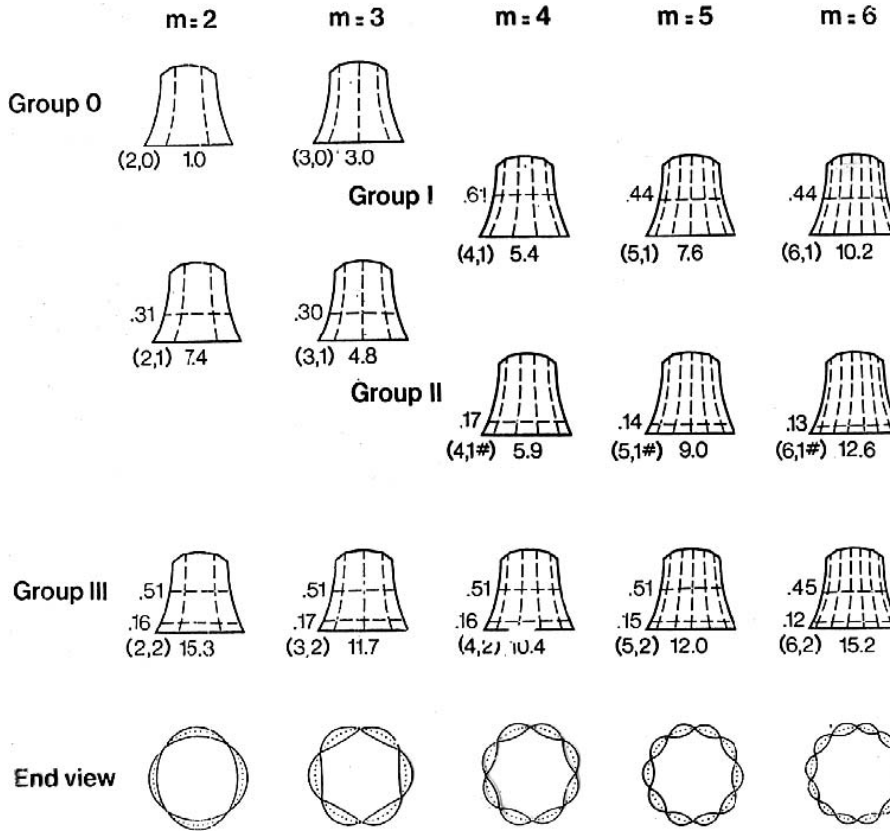

Figure 2.—Systematic grouping of modes of vibration in a hand-bell (from Rossing & Perrin[2]).

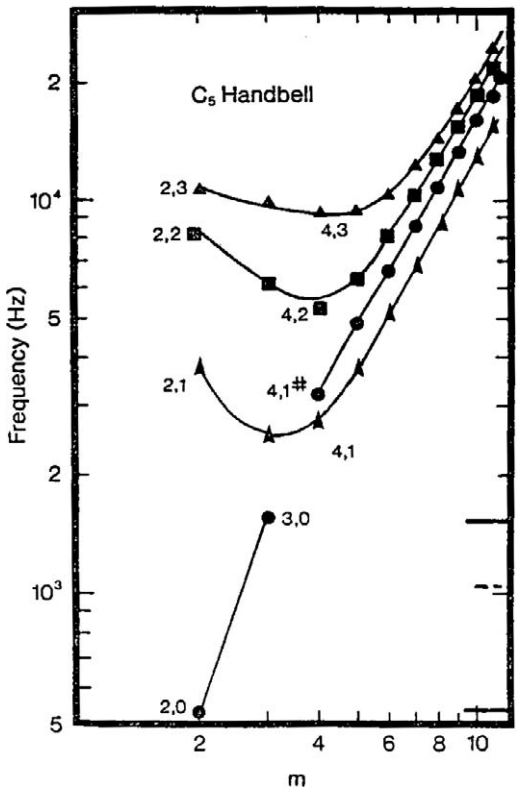

Figure 3.—Relationship of frequency and first mod index of a C_5 Hand-bell (from Rossing, Perrin, Sathoff & Peterson[1]).

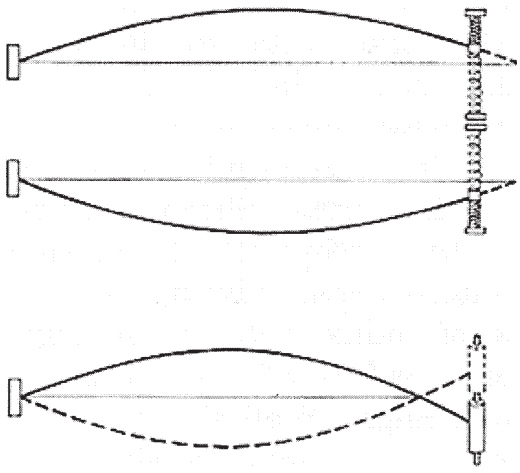

Figure 4.—Relaxing boundary conditions at one end of a vibrating string under tension (from Weinreich[3]).

METHOD

In order to investigate the origin of the (m,$1^{\#}$) modes, models of increasingly complex geometry were studied using Finite Element Analysis (FEA). FEA requires the introduction of geometric and structural parameters including boundary conditions. The former involves imposing a finite number of grid points on the shape of the structure, and the latter requires specifying mechanical and elastic parameters. Values representative of Bronze alloys used for hand-bells were chosen from standard tables. Limits on translational and rotational freedoms for certain parts of the structure are imposed as boundary conditions. For the crudest approximation in the (m,0) mode, a wall section between nodal lines is approximated as a flat rectangular plate of constant wall thickness. The boundary conditions imposed are: clamped at the top, hinged at the sides, and free at the bottom. (figure 5a)

ANSYS^{R}-ED^{TM} [4] an FEA program, commercially available at treasonable cost to students and faculty of educational institutions, provides a large enough number of degrees of freedom to accommodate all increasingly complex approaches to the normal mode hand-bell problem considered in this work. Figure 5a shows the geometry and the mesh chosen for the lowest order of approximation. Figures 5b-d show modes for increasing values of m at increasing frequencies. Clearly the approximation is too crude to illustrate the appearance of the (m,$1^{\#}$) mode. An additional check is made by reducing the plate width. Figures 6a–c again show the inadequacy of the flat rectangular plate model, (m,$1^{\#}$) modes do not appear.

The next approximation takes the rectangle to a trapezoid, reflecting the realization that the circumference of the bell at the mouth is larger than at the crown. Figures 7a–b clearly illustrate that this approximation is still inadequate.

In the next approximation the flat plate is replaced by a curved section of the bell, and again the inadequacy of the model is evidenced in figures 8.

A crown is added for the fourth level of approximation, with the clamped boundary condition imposed near the center of the crown. This modification is still inadequate as shown by figures 9.

For the fifth approximation, an additional curvature, opposite to the curvature added in the third approximation, is introduced.

This approximates the actual bell cross-section more closely. Now the (m,1#) mode appears (fig 10). Imposing a hinged boundary condition at the location of expected nodal lines is difficult for this double curvature configuration, consequently the entire bell is modeled with a fixed thickness contour, and the clamped boundary condition is imposed on the center hole of the crown. Mode (2,1) is shown in fig 11 in gray scale representation. For this configuration modes (2,0), (2,1), (3,1), (4,1) and (3,1#) are shown in figures 12, 13, 14, 15, and 16 respectively. These figures show the extreme displacements of the modes as viewed from the top of the bell.

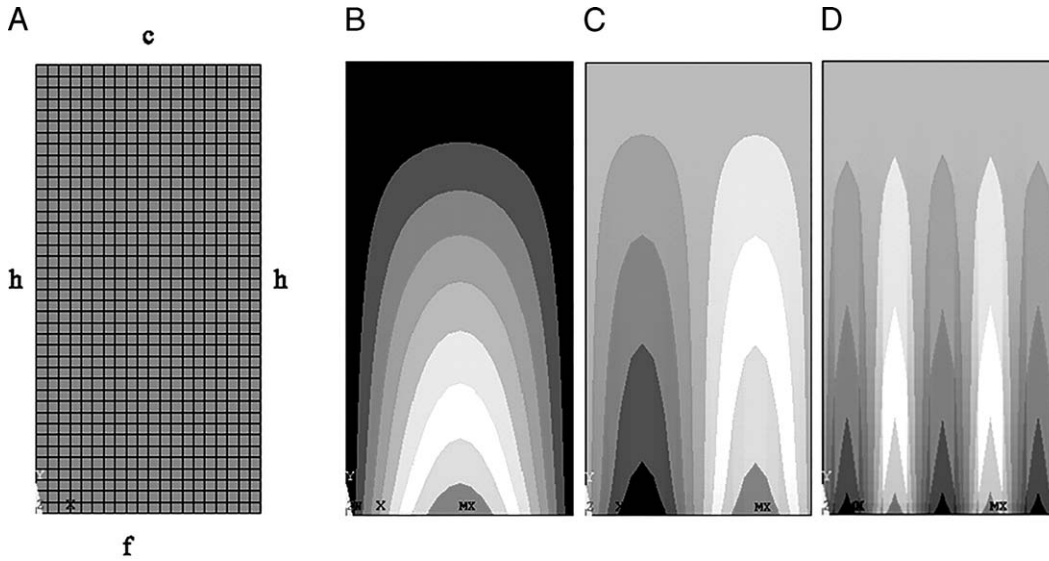

Figure 5.—A. Flat plate with FEA grid and boundary conditions. c—clamped, h—hinged, f—free. B. Mode (0,0). C. Mode (1,0). D. Mode (4,0).

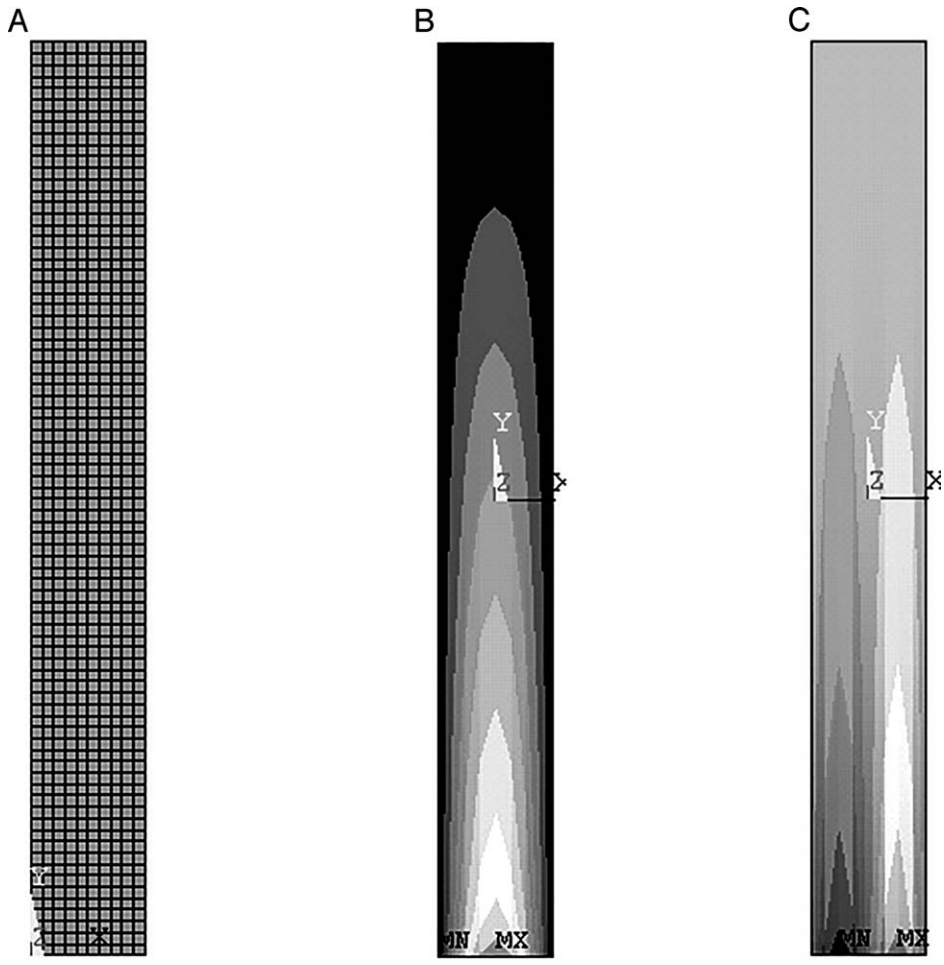

Figure 6.—A. Narrow rectangular plate, same boundary conditions as Figure 5. B. Mode (0,0). C. Mode (1,0).

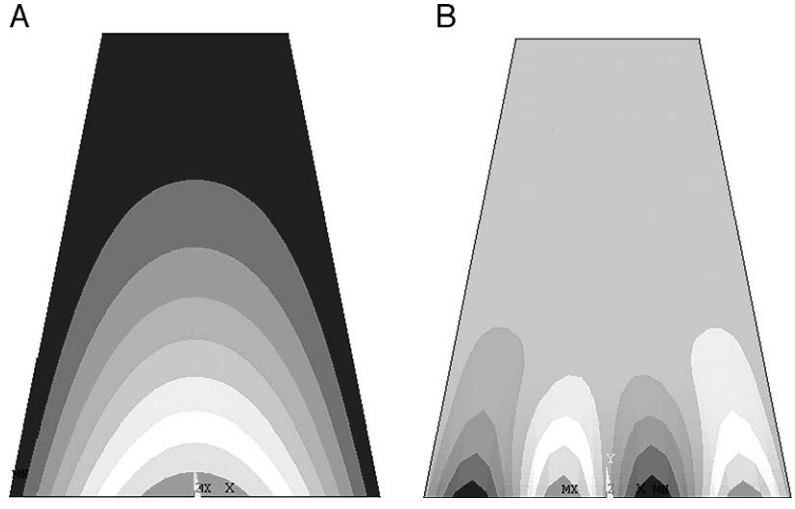

Figure 7.—Flat trapezoidal plate. A. Mode (0,0). B. Mode (3,0).

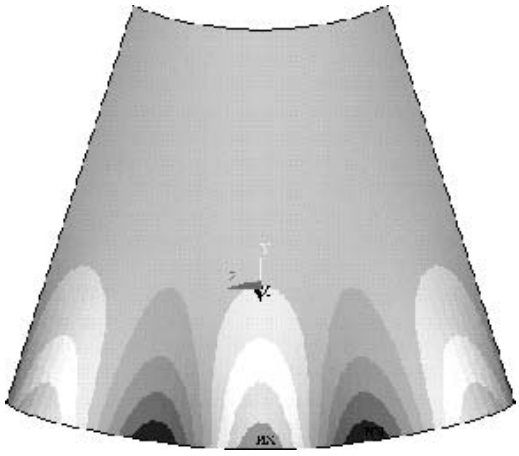

Figure 8.—Conical plate section. Mode (4,0).

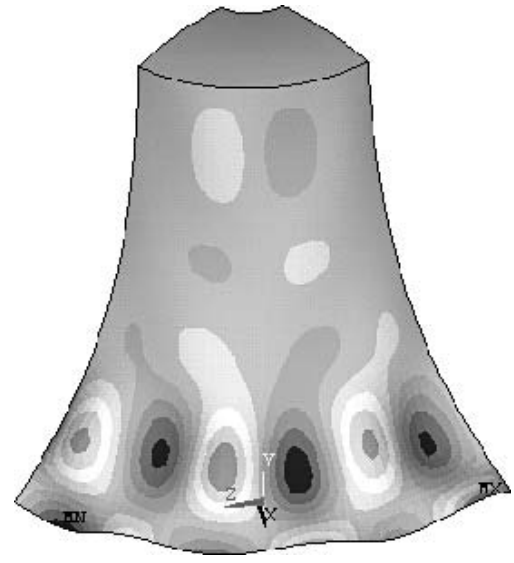

Figure 10.—Bell section with double curvature. Mode (5,1).

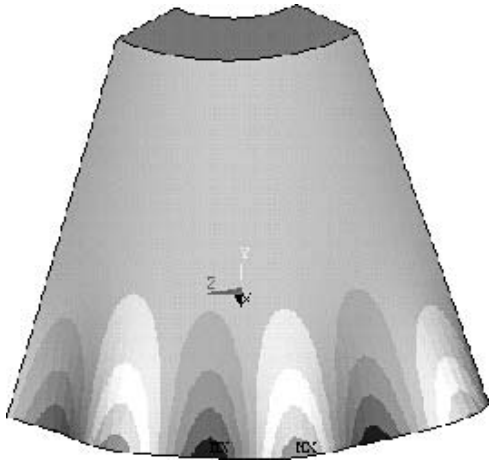

Figure 9.—Conical plate section with crown. Mode (5,0).

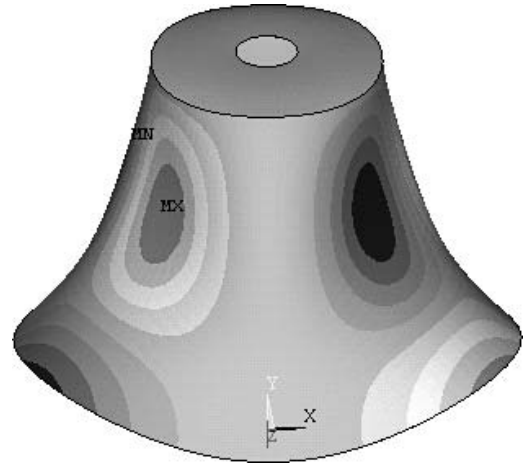

Figure 11.—Bell model. Mode (2,1).

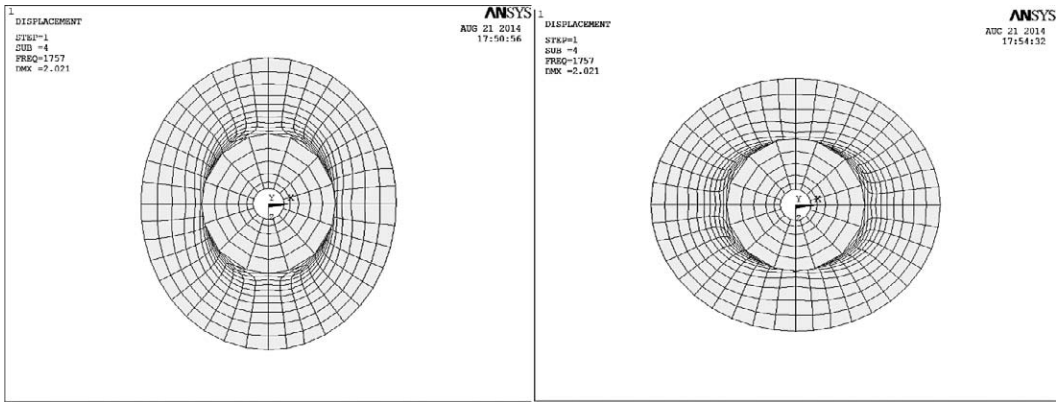

Figure 12.—Two FEA frames of opposite extreme displacement for the (2,0) mode.

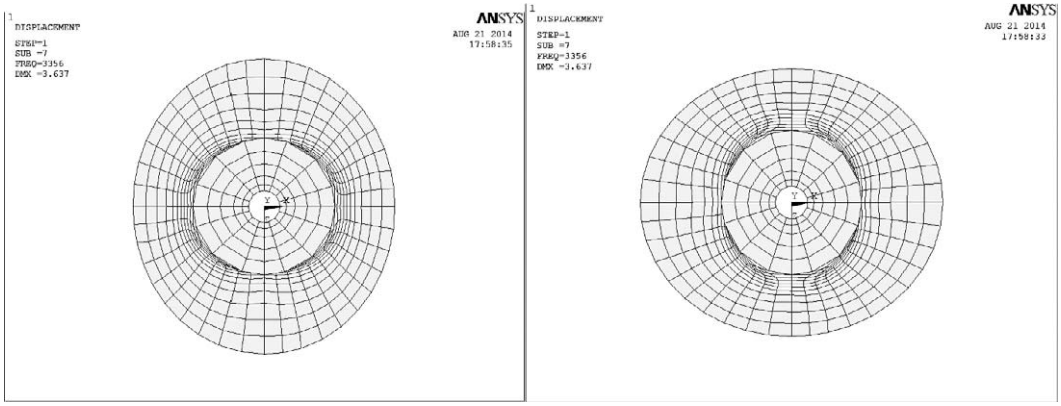

Figure 13.—Two FEA frames of opposite extreme displacement for the (2,1) mode. The nodal line lies approximately between the third and the fourth circumferential grid line.

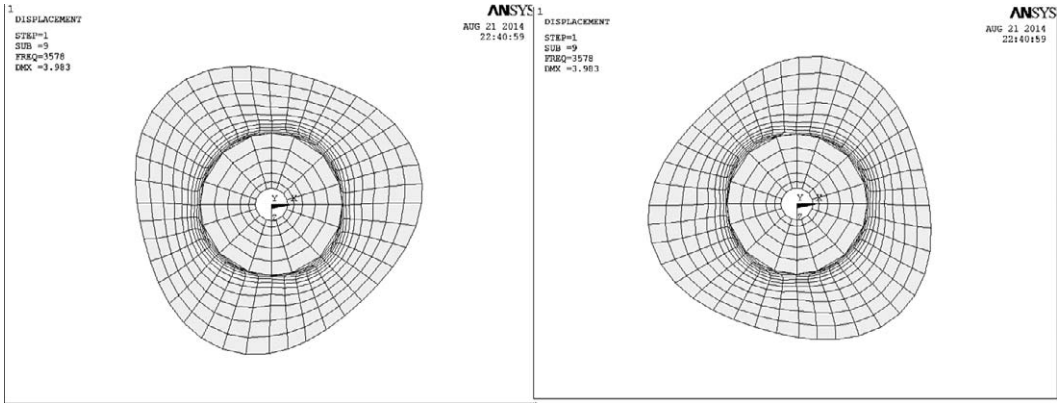

Figure 14.—Two FEA frames of opposite extreme displacement for the (3,1) mode. The nodal line lies approximately between the fourth and the fifth circumferential grid line.

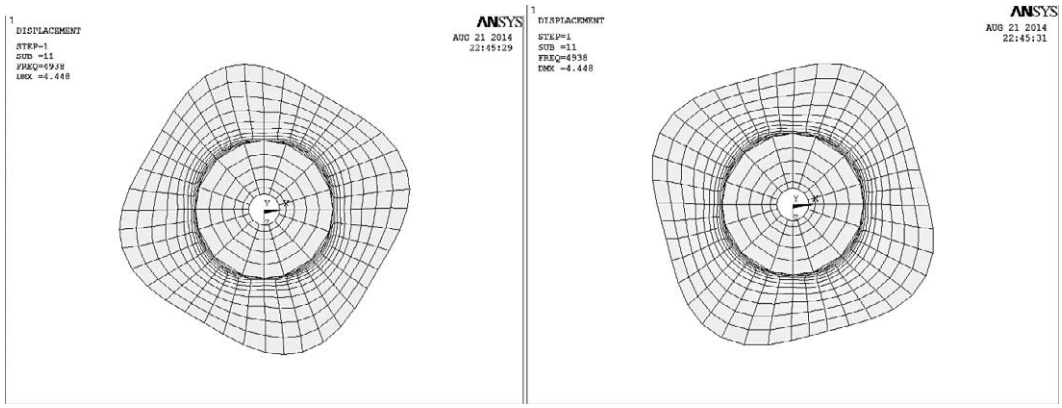

Figure 15.—Two FEA frames of opposite extreme displacement for the (4,1) mode. The nodal line lies approximately between the fourth and the fifth circumferential grid line.

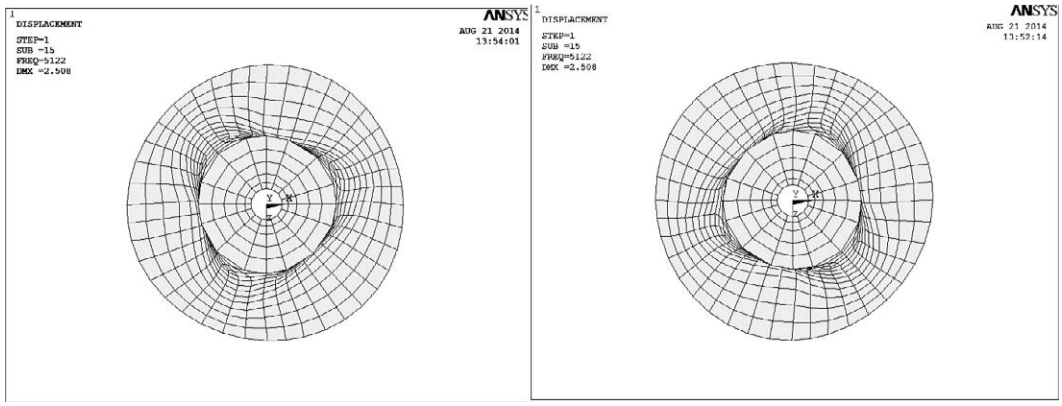

Figure 16.—Two FEA frames of opposite extreme displacement for the (3,1) mode. The nodal line is located between the rim and the first circumferential grid line.

CONCLUSION

From this FEA study of hand-bell models of increasing complexity it appears that the saddle-like double curvature in the side wall of the bell is essential for the formation of the (m,1$^{\#}$) modes. Frequency comparisons with an actual bell are not possible since the cross-section of a real bell would require a full three dimensional FEA model for which the number of degrees of freedom exceed the capability of this program. That study is left for future work with access to a full ANSYS FEA program.

REFERENCES

Rossing, T.D., R. Perrin, H. Sathoff & R.W. Peterson. 1984. Vibrational modes of a tuned handbell. *J. Acoust. Soc. Amer.* 76:Nr. 4, 1263–1267.

Rossing, T.D. & R. Perrin. 1987. Vibrations of Bells. *Applied Acoustics* 20:41–70.

Weinreich, G. Jan 1979. The Coupled Motions of Piano Strings, *Scientific American,* 124.

ANSYS^{R} ED^{TM} ANSYS Inc., Southpointe 275 Technology Dr. Canonsburg, Canonsburg, PA 15317.

Manuscript received 2 October 2013, revised 6 August 2014.